A Review on Numerical Simulation of Multiphase Flows Using the Lattice Boltzmann Method: Emphasis on the Phase-Field Approach

Adithya Aravind[1], Harsh Kumar Rai[2] and Dhiraj Patil[2]

[1]Student, National Institute of Technology, Tiruchirappalli, Summer Intern, Indian Institute of Technology, Dharwad, India

[2]Indian Institute of Technology, Dharwad, India

The numerical simulation of multiphase flows has been a subject of research for a considerable period. The simulation models can be categorized into two distinct types: the sharp interface model and the diffuse interface model. The sharp interface model is plagued by various concerns, including mass conservation, low accuracy of reconstruction, and calculation of surface tension. To overcome these challenges, the diffuse interface model is employed, with a particular focus on the phase-field-based approach. This model is utilized in conjunction with the Lattice Boltzmann Method to enhance the accuracy, simplicity, and physical intuitiveness of these numerical simulations. In this paper, we initiate the discussion of the two main models. The subsequent section will provide a detailed discussion of the Lattice Boltzmann Method. Thereafter, the Phase-field method will be examined in conjunction with the Lattice Boltzmann Method. The next section will include a few test cases performed based on the Lattice Boltzmann method for simple as well as multiphase flows. In the closing sections of the paper, we explore the diverse applications of this method.

Key words: Multiphase flows, Phase-field theory, Computational fluid dynamics

1. Introduction

Multiphase flows have important applications in the fields of engineering and industry. These concepts encompass a diverse range of applications, including but not limited to: fluidized bed reactors, enhanced oil recovery, the examination of boiling and condensation, and the analysis of geophysical flows. The transport processes involved in multiphase flows become intricate due to the various topological changes that occur within the phases and at the interface. The experimental approach facilitated the capture of interface characteristics; however, it lacked precision in its depiction of flow behavior.

Consequently, advancements in the numerical simulation of multiphase flows began to receive attention. Simulations are significantly more cost-effective and can be completed in a substantially shorter timeframe compared to experimental techniques. Consequently, there has been a paradigm shift towards the utilization of numerical modeling and simulation techniques in the study of multiphase flows. As previously discussed, two methods are employed in this field: the sharp-interface and the diffuse-interface models [1]. The sharp-interface model is comprised of three fundamental components: the Volume of Fluid (VoF), the Level Set (LS), and the Front Tracking Methods (FTM) (Wang H., et.al.

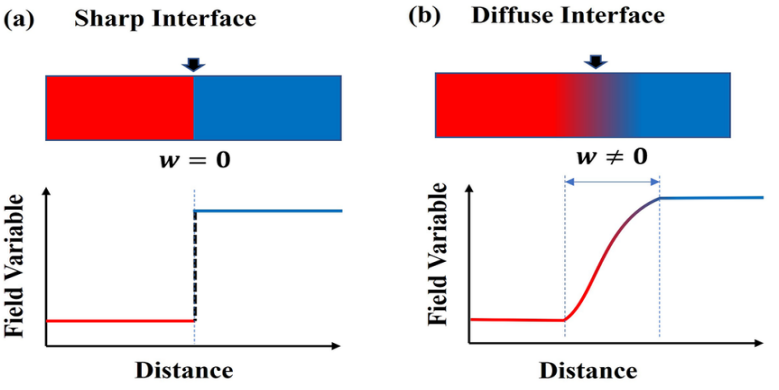

Figure 1. Illustration of the interface in sharp-interface and diffuse-interface models. *Source:* Yuhong Zhao (2024), accessed via: ResearchGate.

2019). The sharp-interface approach considers that the interface has negligible thickness. The physical properties of the two phases undergo a sudden and immediate change at the interface. In the diffuse-interface approach, the zero-thickness interface is replaced by a thin transition zone. This approach serves to mitigate the limitations of the sharp-interface model, as previously delineated. A subset of the diffuse-interface model is the phase-field based approach.

Apart from the traditional approach, the Lattice Boltzmann method is also used for modelling multiphase flows. The Lattice Boltzmann method is based on the kinetic theory and deals with particles on the mesoscopic scale. It uses statistical means to determine the macroscopic parameters such as density, pressure, and velocity. The method introduces a probability distribution function (f) that tells the probability of finding a particle in the phase space. The particles' collision and movement are then modelled to understand their behavior at that scale. Based on this behavior, we get the macroscopic parameters. This method reduces the complexity of the simulation as it does not have to solve any partial differential equations.

There are various models under the Lattice Boltzmann method to specifically solve for multiphase flow problems. They are:

- Color gradient model
- Pseudopotential model
- Free-energy model
- Phase-field-based model

The phase-field-based model is advantageous in that it provides good numerical stability and high accuracy for high-density and high-viscosity multiphase flows. In this model, the Navier-Stokes equations are solved in conjunction with a closure equation, viz., the Cahn-Hilliard equation (CHE) or the Allen-Cahn equation (ACE). The subsequent sections of this paper will provide a more thorough examination of the topics mentioned above.

2. Sharp-Interface and Diffuse-Interface Methods

The commonly used numerical simulation methods for multiphase flows can be classified into two types (Li, J., et.al. 2023):

- Color gradient model
- Pseudopotential model

Among these, the interface-capturing approach is more popular. The subset of the interface-capturing methods includes the sharp-interface and the diffuse-interface methods.

2.1. *Sharp-interface method*

As discussed previously, several methods fall under the sharp-interface category. They are the Volume of Fluid method, the Level Set method, and the Front Tracking method.

The Volume of Fluid method utilizes a mesh to capture the interface. Within the mesh, a scalar function is advected, which aids in the tracking of the interface (Ananthan M., Gaurav T. 2024). This method can capture the changes in complex interfaces. However, it has low accuracy when it comes to reconstruction and ultimately leads to numerical oscillations. The Level Set method introduces a Level Set function (ϕ) or distance function that defines the interface implicitly. This function is continuous. The function can be defined as follows (Ahmad Fawaz, et.al. 2022):

$$\begin{cases} \text{Phase 1 if } \phi < 0 \\ \text{Interface if } \phi = 0 \\ \text{Phase 2 if } \phi > 0 \end{cases}$$

In this method, the surface tension and curvature can be easily calculated. But the function is not preserved and can lead to issues with mass conservation. The Front Tracking Method is grounded on the Lagrangian approach. It has a high order of accuracy. This method can be used to accurately calculate the surface tension and surface energy. The drawback is the inability to capture the topological changes for a complex interface. To address the limitations of the sharp-interface method, the diffuse-interface method was developed.

2.2. *Diffuse-interface method*

The diffuse-interface method can be categorized into two main branches:

- Phase-Field model
- Multi-Fluid model

Under the phase-field model, an order parameter is introduced, which is solved along with a convection-diffusion equation to capture the interface. The macroscopic quantities are then calculated as a function of the order parameter. This model will be discussed in detail in the later sections.

The multi-fluid model considers the interface as diffuse surfaces and allows the artificial mixing between the phases. It has a low computational cost but the trade off is the potential loss in detail while constructing the interface. This model is mainly based on the Volume of Fluid method. The full set of equations are given by Baer-Nunziato's seven equation model (Baer and Nunziato 1986). This consists of two equations for mass conservation, two equations for momentum conservation, two equations for energy conservation, and one equation that defines the type of flow (advection or convection). The generally used models are the subsets of Baer-Nunziato's model, which have been simplified due to the non-conservative nature of the mentioned model. These simplified models are widely used in engineering applications.

The main advantages of the diffuse-interface method over the sharp-interface method are briefly listed as follows (Adebayo, E.M., et.al. 2025):

- Handling of complex interfaces
- Improvement in computational efficiency
- Accurate capture of discontinuities
- Handling abrupt variations in thermodynamic properties

- Minimize spurious numerical oscillations

3. Lattice Boltzmann Method

The Lattice Boltzmann method uses the Kinetic theory and the lattice gas models to statistically determine the positions and velocities of individual particles and represent the macroscopic parameters as a function of these quantities. It assumes that the gases are dilute and composed of point-like particles, the particles interact based on short-range forces, and collisions between the particles are assumed to happen instantaneously.

As mentioned previously, a distribution function is involved that describes the probability density of finding a particle in a phase space. The evolution of this distribution function after the collisions is given by the Boltzmann equation

$$f = f(\mathbf{x}, \mathbf{e}, t) \tag{3.1}$$

where $\mathbf{x}$ is the position and $\mathbf{e}$ is the velocity of the particles.

$$\frac{df}{dt} = \frac{\partial f}{\partial t} + \mathbf{e} \cdot \frac{\partial f}{\partial \mathbf{x}} + \frac{\mathbf{F}}{\rho} \cdot \frac{\partial f}{\partial \mathbf{e}} = \Omega(f) \tag{3.2}$$

where Ω is the collision operator.

Due to the complex nature of the collision operator (omega), it was simplified to the Bhatnagar, Gross, and Krook operator, also known as the BGK operator (Shiyi, et.al. 1998).

$$\Omega(f) = \frac{-(f - f^{eq})}{\tau} \tag{3.3}$$

where τ is the relaxation time. This model is also called the single relaxation time model. The zeroth moment of the equilibrium distribution function with the discrete velocity $\mathbf{e_i}$ gives the density, while the first moment gives the velocity or momentum (Cyrus, et.al. 2010).

Lattice gas models are representations of the mesoscopic particles on a discrete lattice. They are based on statistical mechanics and give us a framework to understand the equilibrium and transport processes that take place at the mesoscopic scale (Lach L. 2025). They are denoted by the General formula $\mathrm{D}_a\mathrm{Q}_b$, where D represents the number of dimensions given by a, and Q represents the number of velocities in the discrete velocity set given by b. The popular two-dimensional lattice models are the D2Q7 and D2Q9 models [2], while for three dimensions, D3Q15 and D3Q19 are common models.

In light of the discrete lattice and the discrete velocities, the Lattice Boltzmann equation is formulated as:

$$f_i(\mathbf{x} + \mathbf{e}_i \Delta t, t + \Delta t) - f_i(\mathbf{x}, t) = \frac{-(f_i(\mathbf{x}, t) - f_i^{eq}(\mathbf{x}, t))}{\tau / \Delta t} \tag{3.4}$$

The equilibrium distribution function is defined by the Maxwell-Boltzmann distribution as:

$$f_i^{eq}(\mathbf{x}, t) = w_i \rho \left(1 + 3\frac{\mathbf{u} \cdot \mathbf{e}_i}{c_s^2} + 9\frac{(\mathbf{u} \cdot \mathbf{e}_i)^2}{2c_s^4} - 3\frac{\mathbf{u} \cdot \mathbf{u}}{2c_s^2}\right) \tag{3.5}$$

where w_i are the weights, ρ is the density, c_s is the speed of sound in the medium, and $\mathbf{u}$ is the speed of the particle.

The above equations describe how collision is modelled in the Lattice Boltzmann method. Subsequently, the boundary conditions are applied to the domain boundaries, and the

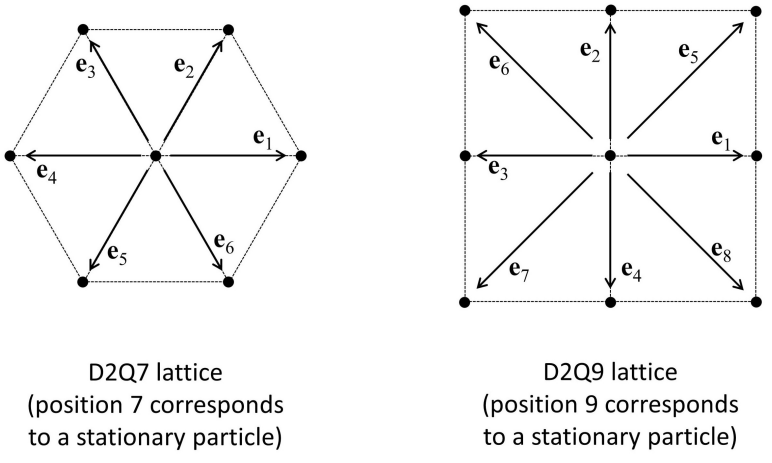

Figure 2. Illustration of the popular 2D lattice gas models; *Source:* Zahid and Cunningham (2025), accessed via: MDPI.

streaming equation is modelled. The boundary conditions can be briefly divided into the velocity boundary conditions, the pressure boundary conditions, and the periodic boundary condition (Robert, et.al. 1996). Within these, the most common boundary conditions applied to the Lattice Boltzmann problems are the no-slip boundary condition, which is also called the bounce-back boundary condition, the periodic boundary condition, the free slip boundary condition, the moving wall boundary condition, and the symmetry boundary condition. Following this general methodology, fluid flow problems are modelled under the Lattice Boltzmann model.

3.1. *LBM for multiphase flows*

When it comes to multiphase flows, the Lattice Boltzmann method follows a similar methodology, but with optimization of the equations that need to be solved for the particular flows. There are primarily four models as mentioned before: the color gradient model, the pseudopotential model, the free-energy model, and the phase-field based model. Each of these models will be discussed in more detail in the upcoming sections.

3.1.1. *Color gradient model*

The color gradient model considers two colors to denote the two phases of the fluid, usually one red and the other blue; in other words, it considers two probability distribution functions. The features of CGM are its ability to represent the two immiscible fluids as sufficiently distinct using the interface thickness parameter, its ability to conserve the momentum locally and globally, and its ability to tune the fluid and flow parameters independently. Following the regular Lattice Boltzmann methodology, two additional steps are added in CGM, namely, "Perturbation" and "Recoloring" (Zahid and Cunningham 2025). The perturbation step assists in enabling interfacial tension into the model, while the recoloring step assists in maintaining the fluids as immiscible. The equation for the perturbation step is given by:

$$(\Omega_i^k)^2 = \frac{A^k}{2}|C|\left[w_i \frac{\mathbf{u}\cdot\mathbf{e}_i}{\mathbf{u}\cdot\mathbf{u}} - B_i\right] \tag{3.6}$$

where A and B are suitable parameters, and C is the color gradient. The equation for the recoloring step is given by:

$$f_i^r(\mathbf{x},t) = \frac{\rho^r}{\rho^t} f_i^t + \left[\beta \frac{\rho^r \rho^b}{(\rho^t)^2} \cos\theta_i\right] f_i^{eq,0} \tag{3.7}$$

$$f_i^r(\mathbf{x},t) = \frac{\rho^b}{\rho^t} f_i^t - \left[\beta \frac{\rho^r \rho^b}{(\rho^t)^2} \cos\theta_i\right] f_i^{eq,0} \tag{3.8}$$

where ρ^r, ρ^b, and $\rho^{tot\cdot}$ are the densities of red region, blue region, and total densities respectively, θ^i represents the angle between the color gradient and the lattice velocity vector, and β is a user-defined parameter.

The main challenges faced by the model include the occurrence of spurious velocities near the interface, inability to model high-density ratio flows, and the inability to eliminate the artificial fluid effects while depicting fluid flow.

3.1.2. *Pseudopotential model*

Also known as the Shan-Chen pseudopotential model (Shan and Chen 1993), this model uses a bottom-up approach, that is, it postulates microscopic interactions between fluid particles. The method is used to simulate multiphase and multicomponent systems. It does not use any interface-tracking or interface-capturing methods.

In this model, the force between the two particles is spatially dependent. Hence, a kernel function was introduced. The force acting between a particle at A and a particle at B can be defined as:

$$\mathbf{F}_{AB} = G(\mathbf{x},\mathbf{x}')\rho(\mathbf{x})\rho(\mathbf{x}')(\mathbf{x}-\mathbf{x}') \tag{3.9}$$

where G is the kernel function, and $\rho(\mathbf{x})$ and $\rho(\mathbf{x}')$ are the number densities at point A and B, respectively.

The number densities are replaced by a new function (ψ) called the pseudopotential function. This is also known as the effective mass at a particular point. Therefore, the final version of the force exerted by point A on point B is given by:

$$\mathbf{F}_{AB} = G(\mathbf{x},\mathbf{x}')\psi(\mathbf{x})\psi(\mathbf{x}')(\mathbf{x}-\mathbf{x}') \tag{3.10}$$

The net force on point x can be written as:

$$\mathbf{F}(\mathbf{x}) = -\int (\mathbf{x}'-\mathbf{x}) G(\mathbf{x},\mathbf{x}')\psi(\mathbf{x})\psi(\mathbf{x}') d^3\mathbf{x}' \tag{3.11}$$

The kernel function is expressed as follows:

$$G(\mathbf{x}) = \begin{cases} G_{SC} & \text{if } |\mathbf{x}-\mathbf{x}'| \le \mathbf{c} \\ 0 & \text{if } |\mathbf{x}-\mathbf{x}'| > \mathbf{c} \end{cases}$$

The pseudopotential function is expressed in a bound as follows:

$$\psi = \rho_0 \left[1 - \exp\left(-\frac{\rho}{\rho_0}\right)\right] \tag{3.12}$$

so that, $0 \le \psi < \rho_0$.

The model is simple and operates on a mesoscopic scale. It falls short when it comes to the tuning of surface tension, and it also contains high spurious velocities. It also faces the limitation of thermodynamic inconsistencies and is limited to low-density and viscosity ratios. To overcome these limitations of the model, several changes have been introduced which can be referred to from (Li Chen, et.al. 2014).

3.1.3. *Free-energy model*

The free energy model is fully based on the principles of thermodynamics, primarily from the free energy perspective. In this approach, at equilibrium, the system is mainly described by a chosen free energy. The collision parameter is dependent on the free energy function Ψ. The model is solved using the free energy function equation along with the Navier-Stokes equation to get the macroscopic variables, notably the non-local pressure.

The free energy equation is given by (Swift, et.al. 1996):

$$\Psi(\mathbf{x}) = \int \left[\psi(T(\mathbf{x}), \rho(\mathbf{x})) + \frac{\kappa}{2}(\nabla\rho(\mathbf{x}))^2\right] \tag{3.13}$$

where ψ is the bulk free energy and κ is the capillary coefficient.

This method boasted an accurate capturing of the interface but was held back due to the Galilean invariance and problems with energy conservation. These shortcomings were brought down due to improvements made towards the model (Petersen, K. J., Brinkerhoff, J. R. 2021).

3.1.4. *Phase-Field based model*

This model comes under the diffuse-interface model. Because the interface is modelled such that the properties change smoothly, there is no need for interface-capturing methods. Instead, the interface is modelled integrally. Diffuse-interface theory claims that in two-phase fluids, mixing is triggered owing to the gradient flow of the chemical potential at the interface. To characterize the phases along the interface, an order parameter (ϕ) is introduced into the model. The next section will discuss the phase-field theory in more detail.

4. Phase-field Theory

As mentioned previously, the Phase-field model is based on the diffuse-interface model. The model is simple and can be compared to the Level Set model. It considers the merits of both the Volume of Fluid method as well as the Level Set method. It also allows the modelling of the properties of the interface. Complex flows can also be simulated using this model. Hence, the phase-field model is very suitable for the numerical simulation of multiphase flows.

The order parameter, used to characterize the phases, is basically any parameter that can distinguish the two phases; that is, something as simple as density can be considered as the order parameter.

4.1. *Two phase flows*

For two-phase flows, the order parameter is given by:

$$\phi = \frac{\rho - \rho_B}{\rho_A - \rho_B}\phi_A + \frac{\rho - \rho_A}{\rho_B - \rho_A}\phi_B \tag{4.1}$$

assuming $\phi_A > \phi_B$

The interface of the mixture is defined as:

$$\Gamma = \left\{\mathbf{x} : \phi(\mathbf{x}, t) = \frac{\phi_A + \phi_B}{2}\right\} \tag{4.2}$$

Using Phase-field theory, the free energy density is given by:

$$f(\phi, \nabla\phi) = \frac{k}{2}|\nabla\phi|^2 + \psi(\phi) \tag{4.3}$$

where the first term is the gradient energy, whereas the second term is the bulk energy, and $\psi(\phi) = \beta(\phi - \phi_A)^2(\phi - \phi_B)^2$ (Lee and Kim 2012; Shen J. 2012).

Based on the above, the mixing energy and chemical potential can be defined by:

$$\begin{aligned} F(\phi, \nabla\phi) &= \int_\Omega f(\phi, \nabla\phi) d\Omega \\ &= \int_\Omega \left[\psi(\phi) + \frac{k}{2} |\nabla\phi|^2 \right] d\Omega \end{aligned} \tag{4.4}$$

and,

$$\begin{aligned} \mu &= \frac{\delta F}{\delta \phi} \\ &= -\nabla \cdot \left(\frac{\partial F}{\partial \nabla \phi} \right) + \frac{\partial F}{\partial \phi} \\ &= -k\nabla^2\phi + \psi'(\phi) \end{aligned} \tag{4.5}$$

where $\psi'(\phi) = 4\beta(\phi - \phi_A)(\phi - \phi_B)(\phi - \frac{\phi_A + \phi_B}{2})$

Assuming that the mixing energy is equivalent to the surface energy, the surface tension can be written as:

$$\sigma = \frac{(\phi_A - \phi_B)^3}{6} \sqrt{2k\beta} \tag{4.6}$$

Next, we will look into the closing equations that can be used in conjunction with the Navier-Stokes equation to procure the solution.

4.1.1. *Cahn-Hilliard equation (CHE) (Cahn and Hilliard 1958, 1959)*

$$\partial_t \phi + \nabla \cdot (\phi \mathbf{u}) = \nabla \cdot (M_\phi \nabla \mu) \tag{4.7}$$

where M_ϕ is the mobility coefficient and $\mathbf{u}$ is the fluid velocity.

4.1.2. *Local Allen-Cahn equation (Local ACE) (Chiu and Lin 2011)*

$$\phi_t + \nabla \cdot (\phi \mathbf{u}) = M_\phi \nabla \cdot \left[\left(1 - \sqrt{\frac{2\beta}{k}} (\phi_A - \phi)(\phi - \phi_B) \frac{1}{|\nabla\phi|} \right) \nabla\phi \right] \tag{4.8}$$

This equation has issues with mass conservation.

4.1.3. *Non-local Allen-Cahn equation (Non-local ACE) (Chai, et.al. 2018b)*

$$\phi_t + \mathbf{u} \cdot \nabla\phi = M_\phi [\nabla^2\phi - \psi' + \beta(t)\sqrt{2\psi}] \tag{4.9}$$

where $\beta(t) = \frac{\int_\Omega \psi' d\mathbf{x}}{\int_\Omega d\mathbf{x}}$.

The mass is conserved using $\frac{d}{dt} \int_\Omega \phi d\mathbf{x} = 0$.

4.1.4. *Navier-Stokes equation (Jacqmin 1999; Kendon, et.al. 2001; Badalassi, et.al. 2003)*

The continuity equation is given by $\nabla \cdot \mathbf{u} = 0$. The momentum conservation equation is formulated as follows:

$$\rho \left(\frac{\partial \mathbf{u}}{\partial t} + \mathbf{u} \cdot \nabla \mathbf{u} \right) = -\nabla p + \nabla \cdot [\rho\nu(\nabla\mathbf{u} + \nabla\mathbf{u}^T)] + F_S + G \tag{4.10}$$

where F_S is the interfacial force and G is the body force.

The interfacial force is given by: $F_S = \mu \nabla \phi$.

In the next section, we look at how to incorporate the local Allen-Cahn and Navier-Stokes equations within the Lattice-Boltzmann model. For incorporating other equations, readers are referred to Wang H., et.al. (2019).

4.2. *Lattice Boltzmann method using Phase-field model*

In this section, we discuss how to use the phase-field model with the Lattice Boltzmann method.

4.2.1. *Lattice Boltzmann model for Local Allen-Cahn equation (Geier, et.al. 2015)*

$$f_i^{eq}(\mathbf{x}, t) = \phi w_i \left(1 + \frac{\mathbf{c}_i \cdot \mathbf{u}}{c_s^2} + \frac{(\mathbf{c}_i \cdot \mathbf{u})^2}{2c_s^4} - \frac{\mathbf{u}_i \cdot \mathbf{u}}{2c_s^2}\right) + \frac{M_\phi \theta}{c_s^2} w_i \cdot \mathbf{c}_i \cdot \mathbf{n} \tag{4.11}$$

where

$$\theta = \sqrt{\frac{2\beta}{k}}(\phi_A - \phi)(\phi - \phi_B)$$
$$M_\phi = c_s^2(\tau_f - 0.5)\Delta t$$
$$\phi = \Sigma_i f_i$$

4.2.2. *Lattice Boltzmann model for incompressible Navier-Stokes equation (Zheng, et.al. 2006)*

$$g_i^{eq} = w_i \left[A_i + \rho \left(\frac{\mathbf{c}_i \cdot \mathbf{u}}{c_s^2} + \frac{(\mathbf{c}_i \cdot \mathbf{u})^2}{2c_s^4} - \frac{\mathbf{u} \cdot \mathbf{u}}{2c_s^2}\right)\right] \tag{4.12}$$

This is the equilibrium distribution function where,

$$A_0 = \frac{9}{4}\rho - \frac{15}{4}\left(\phi\mu + \frac{1}{3}\rho\right)$$
$$A_{1-8} = 3\left(\phi\mu + \frac{1}{3}\rho\right)$$

The force distribution function is given by:

$$R_i = \left(1 - \frac{1}{2\tau_g}\right)\frac{w_i}{c_s^2}\left[(\mathbf{c}_i - \mathbf{u}) + \frac{\mathbf{c}_i \cdot \mathbf{u}}{c_s^2}\mathbf{c}_i\right] \cdot (\mu \nabla \phi + G) \tag{4.13}$$

The macroscopic variables can be calculated using:

$$\rho = \Sigma g_i$$
$$\rho \mathbf{u} = \Sigma \mathbf{c}_i g_i + \frac{1}{2}(\mu \nabla \phi + G)$$

A stable discretization scheme for force in the case of large density ratios was proposed by Lee and Lin (2005), giving the following surface tension:

$$F_s = k\nabla \cdot [(\nabla \rho) \cdot (\nabla \rho)\boldsymbol{I} - (\nabla \rho) \otimes (\nabla \rho)] \tag{4.14}$$

5. Test Cases and Results

In this section, a few benchmark test cases of simple and multiphase flows are performed using the Lattice Boltzmann method, and their results are discussed. The simple flows

are programmed in the language C++, while the multiphase flow problems have been programmed in FORTRAN.

5.1. *Poiseuille flow*

Poiseuille flow is characterized by the flow between two infinitely long parallel and stationary plates separated by a distance [3]. The flow is assumed to be steady, laminar, incompressible, and fully developed. The analytical velocity profile is given by:

$$u(y) = \frac{1}{2\mu}\left(\frac{\partial P}{\partial x}\right) y(H - y) \tag{5.1}$$

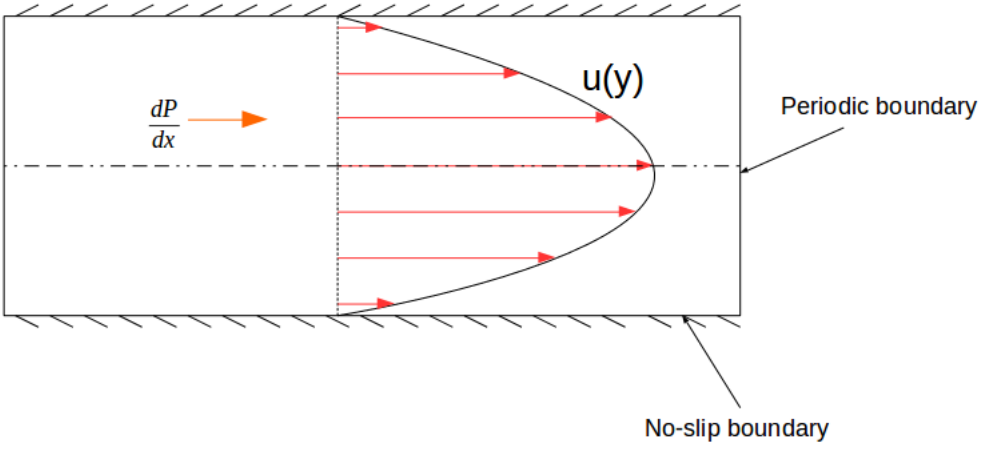

Figure 3. Schematic of Poiseuille flow

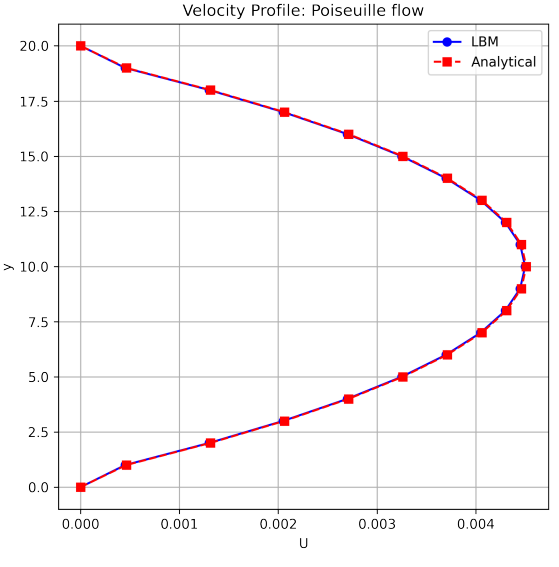

Figure 4. Velocity profile of Poiseuille flow using analytical and LBM approach. The LBM solution matches exactly with analytical solution resulting in an overlapping parabolic profile.

The domain is discretized as a rectangular channel with 200 x 20 grid points. A no-slip boundary condition is applied to the top and bottom walls, while a periodic boundary condition is applied to the left and right walls of the domain. The simulation was run for 20000 time steps. From the figure [4], it can be seen that the solution obtained from the Lattice Boltzmann method exactly matches the analytical solution.

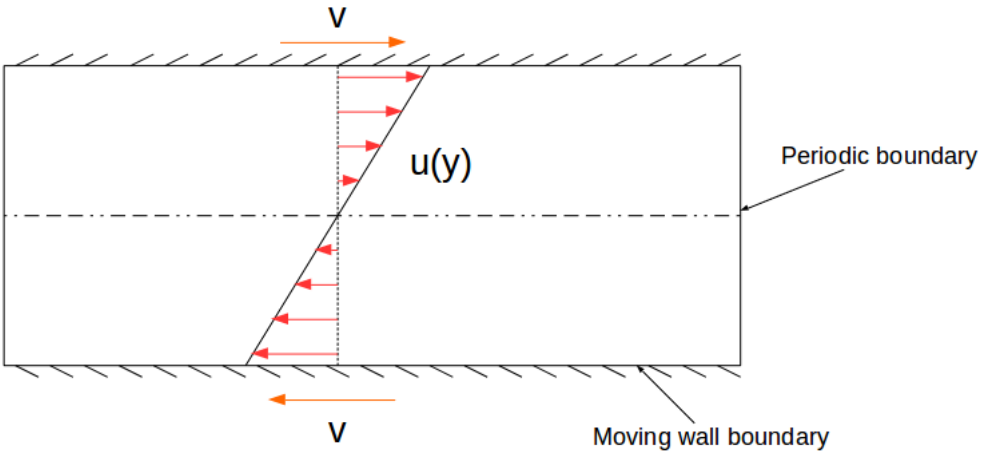

Figure 5. Schematic of Couette flow

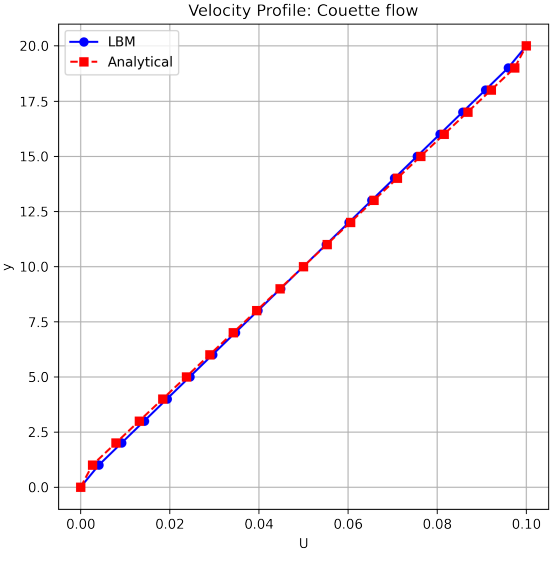

Figure 6. Velocity profile of Couette flow using analytical and LBM approach. The LBM solution matches well and only deviates slightly near the top and bottom walls.

5.2. *Couette flow*

Couette flow is the flow between two infinitely long parallel plates separated by a distance, where one or both plates are moving [5]. The same assumptions as mentioned in Poiseuille

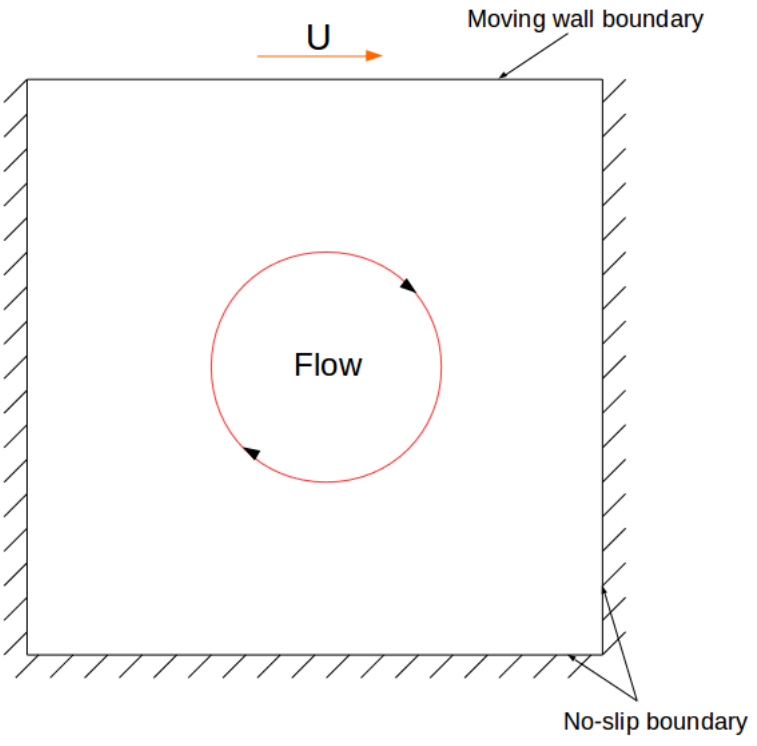

Figure 7. Schematic of Lid driven cavity flow

flow apply to Couette flow. The analytical velocity profile is given by:

$$u(y) = U\frac{y}{H} \tag{5.2}$$

The domain is the same as in the case of Poiseuille flow, and is discretized with 200 x 20 grid points. In this instance, the top plate is given a velocity U and is characterised by a moving wall boundary condition, the bottom plate has a no-slip boundary condition, and the left and right walls are set as periodic boundaries. From figure [6], it can be seen that the Lattice Boltzmann solution is in good agreement with the analytical or the Navier-Stokes solution.

5.3. *Lid driven cavity flow*

The lid-driven cavity flow is a benchmark problem that involves a fluid in a square cavity surrounded by four walls, and the top wall is in motion [7]. This is a two-dimensional flow, depicted by a contour-type plot.

The domain is a square and is discretized by a 20 x 20 grid. The top wall is given a velocity and a moving wall boundary condition. The other three walls are given a no-slip or a bounce-back boundary condition. The velocity contour [8] results in a massive vortex formation in the center of the domain, and is in good agreement with the lid-driven cavity contours found in the literature.

5.4. *Oscillating drop*

The oscillating drop is a fundamental benchmark problem in multiphase flows. The problem encompasses the temporal evolution of a drop due to the viscous and surface tension forces,

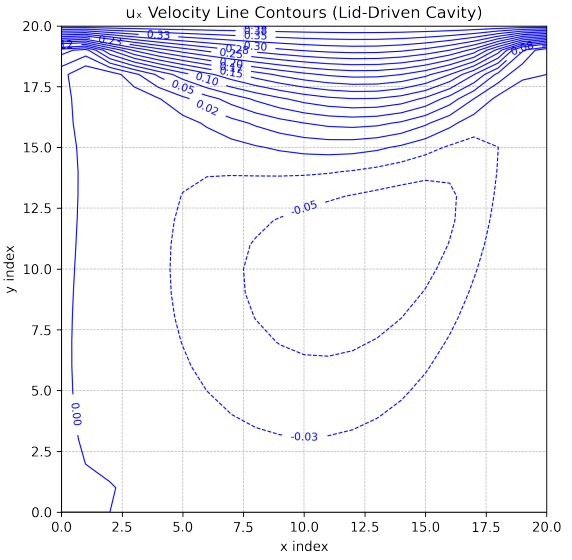

Figure 8. Velocity streamlines for a lid-driven cavity flow for the upper plate moving with velocity 0.4 m/s. The vortices formed in the middle are clearly visible and it deforms towards the direction of movement of the lid.

ultimately bringing the drop into the shape of a circle (2D) with oscillations. This problem is used as a test case to test the stability of a new model.

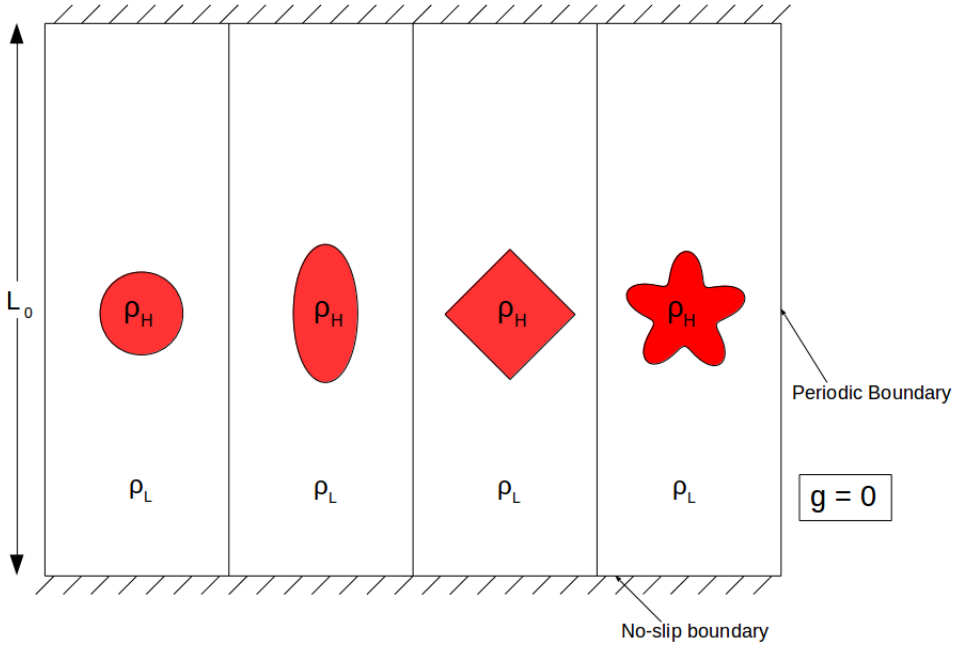

Figure 9. Schematic of Oscillating drop

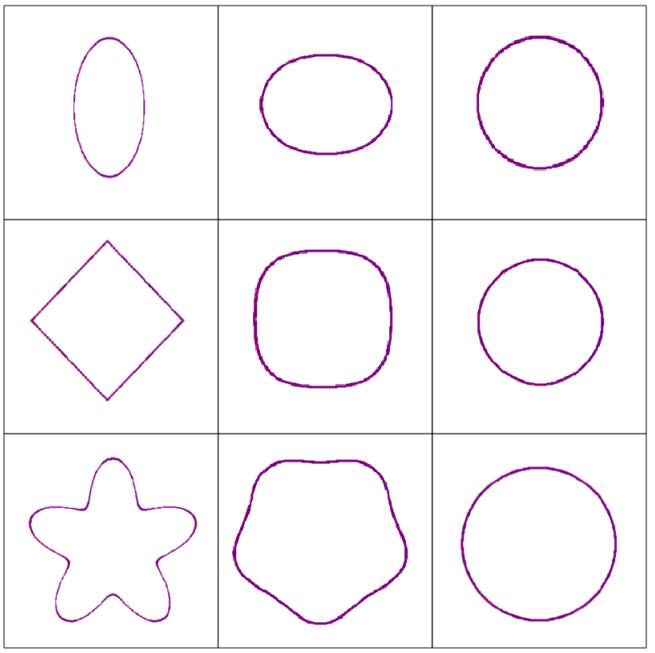

Figure 10. Temporal evolution of an elliptical, a rhombus and a star-shaped drop. The oscillation of the drop takes place between the first and second frames before finally becoming a stable circular shape.

The domain consists of a square, which is discretized into a grid of 256 x 256 nodes, along with an additional ghost node along each dimension. The left and right boundaries were given the periodic boundary condition, whereas the top and bottom walls were given a bounce-back boundary condition [9]. A drop of various shapes was initialized at the center of the domain, and the simulation was run for 1000 time steps. The temporal evolution of an elliptical drop is shown in figure [10].

5.5. *Bubble Rising*

The bubble rising is a crucial benchmark problem that involves the rising characteristics of a bubble under the influence of gravity and its deformation characteristics under the effects of surface tension and viscosity [11]. The rising and deformation characteristics are dependent on three important numbers: the Bond number, the Eötvös number (also known as the Morton number), and the Reynolds number.

These numbers are defined by

$$Bo = \frac{g\rho_h D^2}{\sigma}$$

$$Mo = \frac{g\mu_h^4}{\rho_h \sigma^3}$$

$$Re = \frac{\rho_h U D}{\mu_h}$$

A bubble rising problem was defined with a density ratio of 1000, a viscosity ratio of 100, with $\nu_h = 0.005$ and $\nu_l = 0.05$. The Bond number was taken as 243, the Morton number as 266, and the Reynolds' number as 15.24. The simulation was done for 300000 time steps, and the results are shown in figure [12].

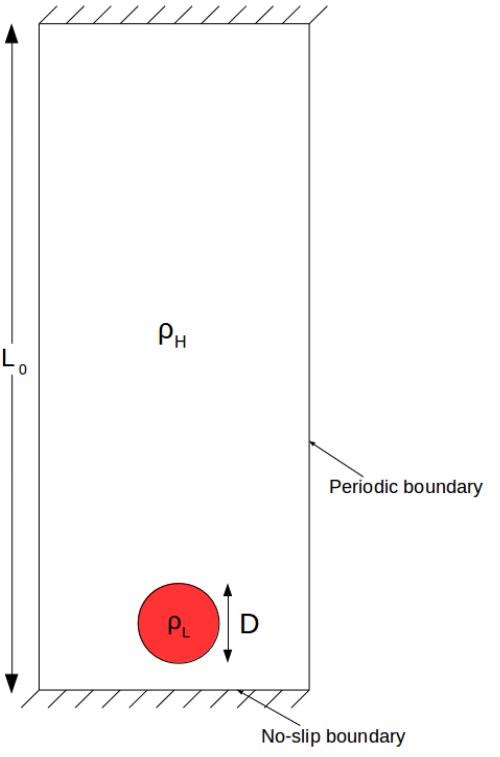

Figure 11. Schematic of Bubble rising

5.6. *Bubble Rising with an obstruction*

This problem is very similar to the previous in the premise that it too involves the rising of a bubble from the bottom in a denser medium, but in this case, there is an obstruction in the path of the bubble [13]. It is also dependent on the three dimensionless numbers. The interaction with the obstruction also depends on the wetting nature of the bubble on the surface.

The bubble can curve around the obstruction, it can separate into two bubbles, or it can also get completely blocked by the obstruction. All this depends on the interplay of four important forces viz., gravitational force, interfacial tension (surface tension), viscous force, and the wetting pressure.

The same parameters as the normal bubble rise was used with the exception of the kinematic viscosity, $\nu_h = 0.0656$ and $\nu_l = 0.656$. A circular obstruction of radius 32 l.u. with non-wetting characteristics is introduced near the bottom of the domain. Similar to the previous problem, the simulation was run for 300000 time steps. The following figure [14] shows the behavior of the bubble around the obstruction.

5.7. *Drop under shear*

The drop under shear is an important test case characterized by a drop placed in a domain between two parallel plates each moving with a velocity in opposite directions. This is synonymous to drop undergoing Poiseuille flow. It leads to an elliptical deformation of the drop along with angular movement or rotation. The schematic of the problem is given in figure [15]. The important dimensionless parameters that characterize the deformation of

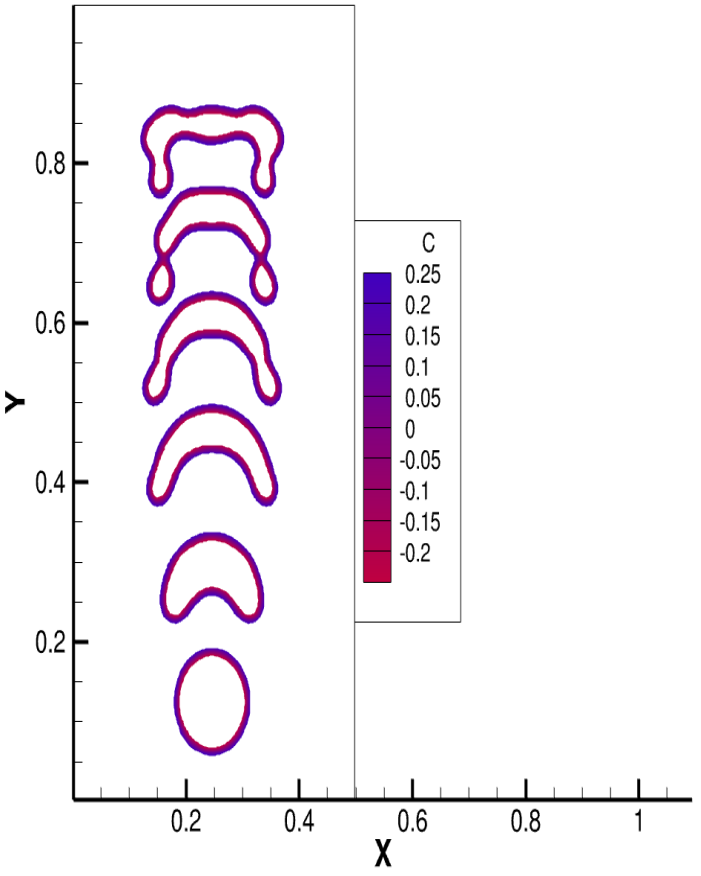

Figure 12. Rising of a bubble in a liquid medium, density ratio 1000 and viscosity ratio 100. The simulation parameters include $Bo = 243, Mo = 266, Re = 15.24$. The bubble deforms due to the heavier liquid above flowing past it as it rises up and forms an inverted-U shape.

the drop under shear are the Capillary number (Ca), the Reynolds number (Re), the Peclet number (Pe), and the viscosity ratio (λ).

A test problem was considered within a domain of 160 x 160 nodes. The dimensionless parameters chosen were as follows: $Re = 0.5, Ca = 0.3, Pe = 0.078$. A circular drop was initialized at the center of the domain. Periodic boundary conditions were applied at the sides and a moving wall boundary condition was applied to the top and bottom walls. The problem was simulated for 1500000 time steps. The deformation experienced by the drop can be seen from figure [16].

6. Applications of multiphase flows and Phase-field method

Multiphase flows have several industrial and scientific applications. Considering industries, they can play a beneficial or an unfavorable role depending on the industry. They play a major role in enhanced oil recovery, especially in water flooding-based recovery and the design of microfluidic devices. Fluidized beds are another industrial application of utmost importance in which solid particles are suspended due to the action of a fluid. These are used mainly in reactors, and their analysis provides valuable information about the

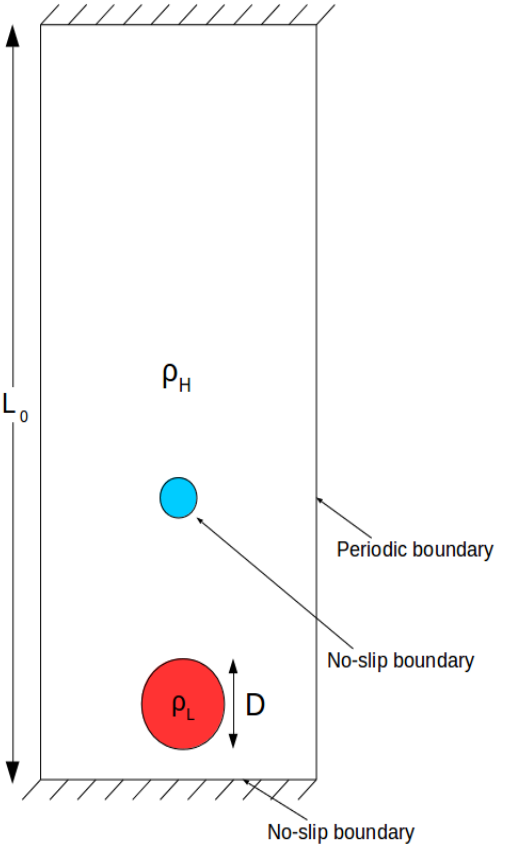

Figure 13. Schematic of Bubble rising with an obstruction

heat transfer capabilities. Alternatively, multiphase flows pose a problem in the case of turbomachinery, like turbines and pumps, in which they might lead to cavitation and erosion of the components due to high density ratios of the fast-moving fluid. In terms of scientific applications, multiphase flows play a crucial role in porous media, microfluidic flows, and the movement of bubbles and droplets. A major application in this domain is the capturing or tracking of the interface, which provides a better understanding of processes such as deformation, breaking, splitting, etc. (Santra S., et.al. 2021). A practical example of the application of multiphase flow is the study of droplet dispersion, particularly in light of the recent COVID-19 pandemic, which can provide important data for understanding the spread of communicable diseases (Shankar S. 2020). Several studies have also been performed on flow through porous media, such as in the soil, which gives an idea about the seepage of water, and also allows us to model the formation of ice during the cold months.

The phase-field method also has advantages in other fields. It is utilized in the study of crack propagation, hydraulic fracturing, bubble behavior, liquid droplets, coalescing, and the separation of microbubbles. It is also used to simulate particles for inkjet printing, model biofilm formation, predict cell growth, and model large-scale structures. Some examples include the numerical study of crack propagation in poroelastic porous media by Zhou, et.al. (2019), hydraulic fracturing and cracking in a non-homogeneous fluid saturated porous media was simulated by Xia, et.al. (2017), a novel method for analyzing

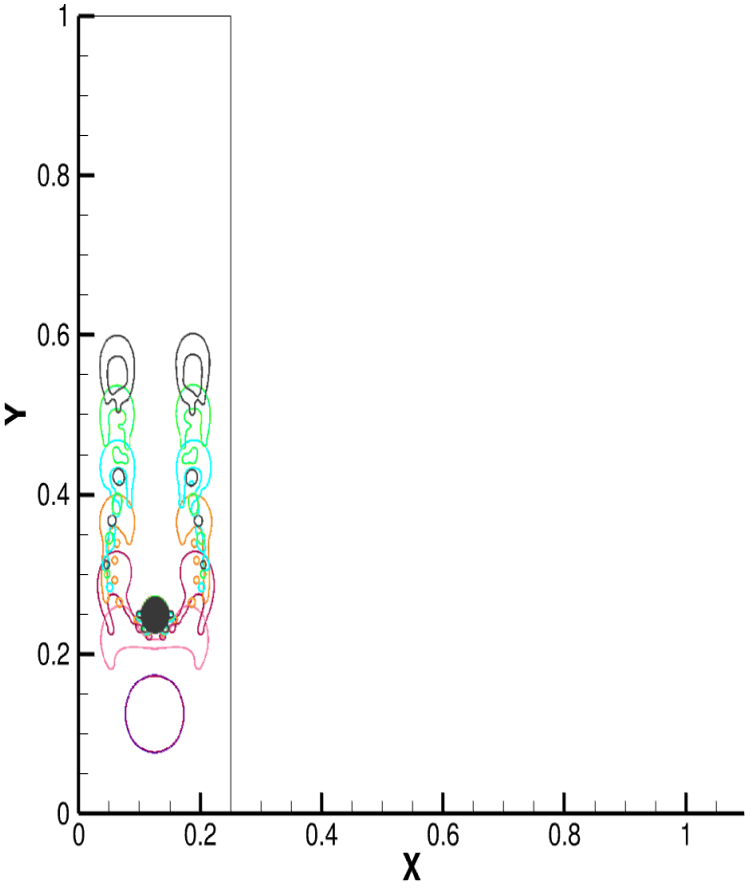

Figure 14. Rising of a bubble in a liquid medium with an obstruction with non-wetting characteristics, density ratio 1000 and viscosity ratio 100. The simulation parameters are $Bo = 243, Mo = 266, Re = 15.24$. The bubble traps the heavier fluid between itself and the obstruction and later splits into two satellite bubbles.

the ductile fracture of elasto-plastic material in a quasistatic linear regime was proposed by Ambati, et.al. (2015), among others.

7. Conclusion

In this paper, we have reviewed the various methods for the numerical simulation of multiphase flows. The traditional numerical approach can be briefly divided into two: the sharp interface and the diffuse interface approach. Each of these approaches has several models within it with specific advantages and challenges.

To summarize the models, the sharp interface method contains the Volume of Fluid method, the Level Set method, and the Front Tracking Method. The diffuse interface method consists of the phase-field based method and the multi-fluid method.

Apart from these traditional methods, the Lattice Boltzmann method plays a crucial role in simulating multiphase flows. It provides a simpler and more robust as well as accurate model, which saves a lot of computational time and effort. The various types of Lattice Boltzmann method include the color gradient method, the pseudopotential method, the free energy method, and the phase-field based method. Among these, the phase-field method is

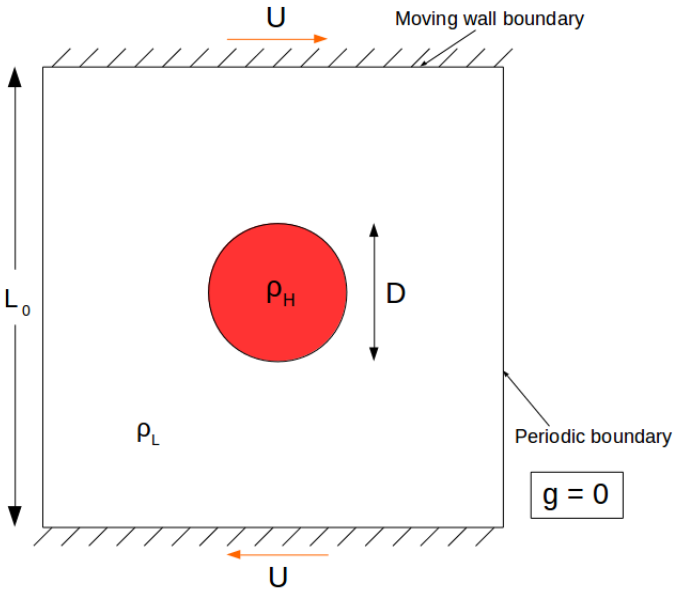

Figure 15. Schematic of Drop under shear

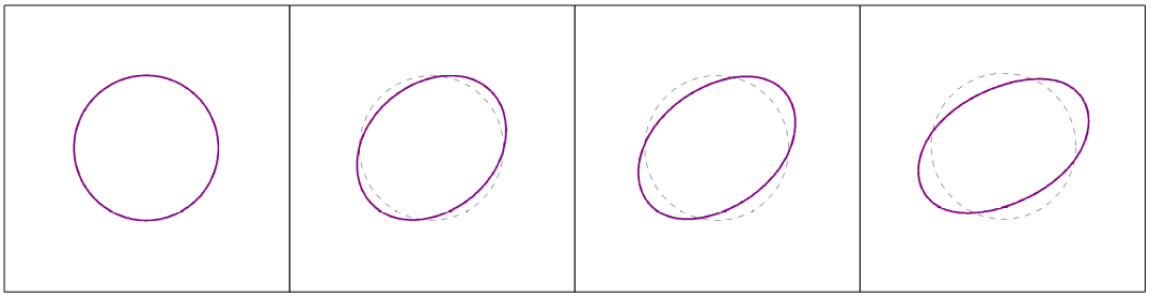

Figure 16. Drop under shear considering a shear rate of $6.25e^{-4}$. The simulation parameters include $Re = 0.5, Ca = 0.3, Pe = 0.078$. Both density and viscosity ratio are 1. The drop which is initialized as a circle deforms into an ellipse at an angular orientation.

simple as well as accurate in capturing the interface, and the later models do not possess Galilean invariance. Hence, PFM is widely used in a large number of engineering and research applications, from the petroleum industry and materials to droplet and bubble behavior.

References

Li Chen, Qinjun Kang, Yutong Mu, Ya-Ling He, Wen-Quan Tao 2014 A critical review of the pseudopotential multiphase lattice Boltzmann model: Methods and applications, *International Journal of Heat and Mass Transfer*, Volume 76, pp. 210-236, https://doi.org/10.1016/j.ijheatmasstransfer.2014.04.032

Robert S. Maier, Robert S. Bernard, Daryl W. Grunau 1996 Boundary conditions for the lattice Boltzmann method, *Physics of Fluids*, 8(7), pp. 1788–1801, https://doi.org/10.1063/1.868961.

Aidun, Cyrus K. and Clausen, Jonathan R. 2010 Lattice-Boltzmann Method for Complex Flows, *Annual Review of Fluid Mechanics*, Volume 42, pp. 439-472 https://doi.org/10.1146/annurev-fluid-121108-145519.

Chen, Shiyi and Doolen, Gary D. 1998 Lattice Boltzmann Method for Fluid Flows, *Annual Review of Fluid Mechanics*, Volume 30, pp. 329-364 https://doi.org/10.1146/annurev.fluid.30.1.329.

Ahmad Fawaz, Yuchao Hua, Steven Le Corre, Yilin Fan, Lingai Luo 2022 Topology optimization of heat exchangers: A review, *Energy*, Volume 252, https://doi.org/10.1016/j.energy.2022.124053.

Wang, H., Yuan, X., Liang, H., Chai, Z., Shi, B. 2019 A brief review of the phase-field-based lattice Boltzmann method for multiphase flows, *Capillarity* 2(3) pp. 33-52 doi: 10.26804/capi.2019.03.01.

Petersen, K. J., Brinkerhoff, J. R. 2021 On the lattice Boltzmann method and its application to turbulent, multiphase flows of various fluids including cryogens: A review, *Physics of Fluids*, Volume 33, https://doi.org/10.1063/5.0046938

Li, J., Zheng, D., Zhang, W. 2023 Advances of Phase-Field Model in the Numerical Simulation of Multiphase Flows: A Review, *Atmosphere, 14*, https://doi.org/10.3390/atmos14081311.

Lach, L. 2025 Phase Stability and Transitions in High-Entropy Alloys: Insights from Lattice Gas Models, Computational Simulations, and Experimental Validation, *Entropy,* **27**, https://doi.org/10.3390/e27050464

Zahid, F., Cunningham, J.A. 2025 Review of the Color Gradient Lattice Boltzmann Method for Simulating Multi-Phase Flow in Porous Media: Viscosity, Gradient Calculation, and Fluid Acceleration, *Fluids, 10*, https://doi.org/10.3390/fluids10050128

Adebayo, E.M., Tsoutsanis, P., Jenkins, K.W 2025 A Review of Diffuse Interface-Capturing Methods for Compressible Multiphase Flows, *Fluids, 10*, https://doi.org/10.3390/fluids10040093

Michael R. Swift, E. Orlandini, W. R. Osborn, and J. M. Yeomans 1996 Lattice Boltzmann simulations of liquid-gas and binary fluid systems, *Phys. Rev. Lett.*, 75(5): 830.

Ananthan M., Gaurav T. 2024 Volume of Fluid Method: A Brief Review, *J. Indian Inst. Sci.*, Vol. 104:1, pp. 229-248.

Zhao, Yuhong 2024 Integrated unified phase-field modeling (UPFM), *Materials Genome Engineering Advances*, **2**, doi: 10.1002/mgea.44

Jacqmin, D. 1999 Calculation of two-phase Navier-Stokes flows using phase-field modeling, *J. Comput. Phys.*, 155(1), pp. 96-127

Lee, H., Kim, J. 2012 An efficient and accurate numerical algorithm for the vector-valued Allen-Cahn equations, *Comput. Phys. Commun.*, 183, pp. 2107-2115, https://doi.org/10.1016/j.cpc.2012.05.013

Shen, J. 2012 Modeling and numerical approximation of two-phase incompressible flows by a phase-field approach, *Multiscale Modeling And Analysis For Materials Simulation*, https://doi.org/10.1142/9789814360906_0003

Chiu, P.H., Lin, Y.T. 2011 A conservative Phase-field method for solving incompressible two-phase flows, *J. Comput. Phys.*, 230(1), pp. 185-204, https://doi.org/10.1016/j.jcp.2010.09.021

Geier, M., Fakhari, A., Lee, T. 2015 Conservative phase-field lattice Boltzmann model for interface tracking equation, *Phys. Rev. E*, 91(6): 063309, https://doi.org/10.1103/PhysRevE.91.063309

Chai, Z., Sun, D., Wang, H., et al. 2018b A comparative study of local and nonlocal Allen-Cahn equations with mass conservation, *Int. J. Heat Mass Transf.*, 122, pp. 631-642, https://doi.org/10.1016/j.ijheatmasstransfer.2018.02.013

Kendon, V.M., Cates, M.E., Pagonabarraga, I., et al. 2001 Inertial effects in three-dimensional spinodal decomposition of a symmetric binary fluid mixture: A lattice Boltzmann study, *J. Fluid Mech.*, 440, pp. 147-203, https://doi.org/10.1017/S0022112001004682

Badalassi, V.E., Ceniceros, H.D., Banerjee, S. 2003 Computation of multiphase systems with Phase-field models, *J. Comput. Phys.*, 190, pp. 371-397, https://doi.org/10.1016/S0021-9991(03)00280-8

Zheng, H., Shu, C., Chew, Y.T. 2006 A lattice Boltzmann model for multiphase flows with large density ratio, *J. Comput. Phys.*, 218(1), pp. 353-371, https://doi.org/10.1016/j.jcp.2006.02.015.

Cahn, J.W., Hilliard, J.E. 1958 Free energy of a nonuniform system. I. Interfacial free energy, *J. Chem. Phys.*, 28(2), pp. 258-267.

Cahn, J.W., Hilliard, J.E. 1959 Free energy of a nonuniform system. III. Nucleation in a two-component incompressible fluid, *J. Chem. Phys.*, 31(3), pp. 688-699.

Zhou, S.W., Zhuang, X.Y., Rabczuk, T. 2019 Phase-field modeling of fluid-driven dynamic cracking in porous media, *Comput. Methods Appl. Mech. Eng.*, 350, pp. 169–198, https://doi.org/10.1016/j.cma.2019.03.001

Xia, L., Yvonnet, J., Ghabezloo, S. 2017 Phase-field modeling of hydraulic fracturing with interfacial damage in highly heterogeneous fluid-saturated porous media, *Eng. Fract. Mech.*, 186, pp. 158–180, https://doi.org/10.1016/j.engfracmech.2017.10.005

Ambati, M., Gerasimov, T., De, L.L. 2015 Phase-field modeling of ductile fracture, *Comput. Mech.*, 55, pp. 1017–1040, https://doi.org/10.1007/s00466-015-1151-4

M.R. Baer, J.W. Nunziato 1986 A two-phase mixture theory for the deflagration-to-detonation transition (ddt) in reactive granular materials, *International Journal of Multiphase Flow*, Volume 12, Issue 6, pp. 861-889, https://doi.org/10.1016/0301-9322(86)90033-9

Lee, T., Lin, C.L. 2005 A stable discretization of the lattice Boltzmann equation for simulation of incompressible two-phase flows at high density ratio, *J. Comput. Phys.*, 206(1), pp. 16–47, https://doi.org/10.1016/j.jcp.2004.12.001

Shan, X., Chen, H. 1993 Lattice Boltzmann model for simulating flows with multiple phases and components, *Phys. Rev. E*, Volume 47, Issue 3, pp. 1815–1819, https://doi.org/10.1103/PhysRevE.47.1815

Shankar Subramaniam 2020 Multiphase flows: Rich physics, challenging theory, and big simulations, *Phys. Rev. Fluids*, Volume 5, Issue 11, pp. 110520, https://doi.org/10.1103/PhysRevFluids.5.110520

Santra, S., Mandal, S. and Chakraborty, S. 2021 Phase-field modeling of multicomponent and multiphase flows in microfluidic systems: a review, *International Journal of Numerical Methods for Heat & Fluid Flow*, Vol. 31, No. 10, pp. 3089-3131, https://doi.org/10.1108/HFF-01-2020-0001